



HAL
open science

Solvent-Induced Aggregation of Self-Assembled Copper–Cysteine Nanoparticles Reacted with Glutathione: Enhancing Linear and Nonlinear Optical Properties

Dipankar Bain, Isabelle Russier-Antoine, Hao Yuan, Sarita Kolay, Sylvain Maclot, Christophe Moulin, Estelle Salmon, Pierre-François Brevet, Anna Pniakowska, Joanna Olesiak-Bańska, et al.

► **To cite this version:**

Dipankar Bain, Isabelle Russier-Antoine, Hao Yuan, Sarita Kolay, Sylvain Maclot, et al.. Solvent-Induced Aggregation of Self-Assembled Copper–Cysteine Nanoparticles Reacted with Glutathione: Enhancing Linear and Nonlinear Optical Properties. *Langmuir*, 2023, 39 (46), pp.16554-16561. 10.1021/acs.langmuir.3c02526 . hal-04386809

HAL Id: hal-04386809

<https://hal.science/hal-04386809>

Submitted on 15 Jan 2024

HAL is a multi-disciplinary open access archive for the deposit and dissemination of scientific research documents, whether they are published or not. The documents may come from teaching and research institutions in France or abroad, or from public or private research centers.

L'archive ouverte pluridisciplinaire **HAL**, est destinée au dépôt et à la diffusion de documents scientifiques de niveau recherche, publiés ou non, émanant des établissements d'enseignement et de recherche français ou étrangers, des laboratoires publics ou privés.

Solvent-Induced Aggregation of Self-Assembled Copper-Cysteine Nanoparticles Reacted with Glutathione: Enhancing Linear and Nonlinear Optical Properties.

Dipankar Bain¹, Isabelle Russier-Antoine¹, Hao Yuan¹, Sarita Kolay^{1,2}, Sylvain Maclot¹, Christophe Moulin¹, Estelle Salmon¹, Pierre-François Brevet¹, Anna Pniakowska³, Joanna Olesiak-Bańska³, and Rodolphe Antoine^{1*}

¹ Institut Lumière Matière, University of Lyon, Université Claude Bernard Lyon 1, CNRS, F-69622 Lyon, France

^{1,2}School of Materials Sciences, Indian Association for the Cultivation of Science, Kolkata 700032, India.

³Institute of Advanced Materials, Wrocław University of Science and Technology, 50-370 Wrocław, Poland

Corresponding Author: Rodolphe Antoine, **Email :** rodolphe.antoine@univ-lyon1.fr

Abstract:

Copper-thiolate self-assembly nanostructures are unique class of nanomaterials because of their interesting properties such as hierarchical structures, luminescence, and large nonlinear optical efficiency. Herein, we synthesized bio-molecules cysteine (Cys) and glutathione (GSH) capped sub-100 nanometer self-assembly nanoparticles (Cu-Cys-GSH NPs) with red fluorescence. The as-synthesized NPs show high emission enhancement in presence of ethanol, caused by the aggregation-induced emission (AIE). We correlated the structure and optical properties of Cu-Cys-GSH NPs by measuring the mass, morphology and surface charge as well as their two-photon excited fluorescence cross-section (σ_{2PEPL}), two-photon absorption cross-section (σ_{TPA}) and first hyperpolarizability (β) of Cu-Cys-GSH NPs in water and water-ethanol using near-infrared (NIR) wavelength. We found high β value as $(77\pm 10) \times 10^{-28}$ esu (in water) compared to the reference medium water. The estimated value of σ_{2PEPL} and σ_{TPA} are found to be 13 ± 2 GM and $1.4\pm 0.2 \times 10^4$ GM, respectively. We hope our investigations of linear and nonlinear optical properties of copper-thiolate self-assemblies in water and its solvent induced aggregates will open up new possibilities in designing self-assembled systems for many applications including sensing, drug delivery and catalysis.

Introduction

Supramolecular nano-assemblies exclusively formed from ligand-protected noble metals (NMs) are attracting much attention due to their unique properties arising from their well-organized structure.^{1, 2} Specific organization in polymeric chains are particularly rich when ligands possess a thiol (-S-H) group inducing various interactions: metal-sulfur coordination, metallophilic interactions between NM atoms as well as interactions at the ligands interface: H-bonding, electrostatic and hydrophobic interactions. The -S-H-containing amino acids and peptides such as cysteine (Cys), homocysteine (Hcys), and glutathione (GSH) are good candidates to produce hybrid noble metal-based materials with well-organized structures and rich optical properties, in particular strong chiroptical properties due to the chiral nature of biomolecules. For instance, the hierarchical assembly structure of Au-cysteine (Au-Cys) particles has recently attracted attention because of their surprising chiroptical properties, chemical properties, even higher complexity than biological counterparts.³ The hierarchy emerges from the subnanometric -Au-S- chains, and the intertwined inter- or intra-chain -Au-Au- metallophilic interactions connecting different chains to form structures with greater complexity.⁴ Antoine and collaborators reported unique formation of helices leading to strong circular dichroism of Au(I)-Cys driven by the hierarchical structure formed from supramolecular self-assembly.^{5, 6} They also explored the interplay of electrostatic interactions between cysteine ligands and metallophilic attraction in the polymeric backbone of Au(I)-Cys.⁶ Incorporation of foreign metals in such nanomaterials enhances several of their properties such as nonlinear optical and chiroptical properties.⁷ In particular, silver-doping was used as a strategy to enhance the optical properties of helical gold-cysteine supramolecular assemblies.⁵

In addition to Au(I)-Cys systems, it is expected that the M(I)-SR coordination polymers (M = Cu, Ag, or Au) could in general function as spectral sensing ensembles for extended applications. Chiroptical activity of silver-cysteine (Ag(I)-Cys), associated with formation of polymeric species, has been studied in the perspective of development of new sensing systems.^{8, 9} Copper forms a rich variety of compounds, usually with oxidation states +1 and +2, which are called cuprous and cupric, respectively. In the cuprous form, a copper thiolate lamellar coordination polymer, [Cu(p-SPhCO₂Me)]_n has been described featuring an unprecedented photoluminescence¹⁰ useful for thermochromic luminescence.¹¹ Yin et al. have synthesized a highly luminescent Cu(I)-GSH complex which shows intense red fluorescence owing to ligand to metal charge transfer between GSH and copper.¹² In addition Zheng and

coworkers demonstrated the successful syntheses of homochiral Cu(I) coordination polymers with a unique double-stranded helical building block from achiral precursors via symmetry-breaking crystallization.¹³ The cupric form of copper has also a rich interaction with cysteine containing biomolecules. It was found that Cu(II) complexed with cysteine formed cage-like clusters.¹⁴ Ma et al. synthesized copper-cysteine mercaptide nanoparticles (Cu-Cys NPs) via a facile coordination process between copper Cu(II) ions and the sulfhydryl groups of L-cysteine in an alkaline solution.¹⁵ Indeed, in the alkaline aqueous solution, L-cysteine first coordinated with Cu(II) to generate Cys-Cu-Cys mercaptide molecules through Cu-S coordination. With increasing concentration, the water-insoluble Cys-Cu-Cys molecules gradually self-assemble and form sub-100 nm Cu-Cys NPs (see scheme 1).



Scheme 1. Schematic representation of Cu-Cys self-assembled nanoparticles synthesis.

Such sub-100 nm Cu-Cys NPs are non-luminescent and were used for in situ glutathione-activated and H₂O₂-reinforced chemodynamic therapy for drug-resistant breast cancer.¹⁵ Tuning optical properties in particular photoluminescence (PL) can be obtained by the regulation of noncovalent interaction inside nanostructures. A first strategy consists in playing with solvent polarity. Previous studies revealed that weakly polar solvent could strengthen the intermolecular interaction between AIE-type NCs, leading to aggregation and improving fluorescence.¹⁶ Tuning silver-based nanoclusters emission from orange to blue was obtained by the regulation of solvent-induced noncovalent interactions inside nanostructures.¹⁷ On the other hand, ligand strategy could strikingly improve the PL properties by introducing a capping layer, restricting the intramolecular vibration and rotation of the components of the non-luminescent particles. Such a strategy was nicely demonstrated to enhance the luminescence,

both in the linear^{18, 19} and nonlinear optical²⁰ regimes of 6-aza-2-thiothymine-stabilized AuNPs (ATT-AuNPs) by introducing L-arginine into the capping layer.

In this work, starting with sub-100 nm Cu-Cys NPs, we further explore the ligand and solvent strategy to enhance their optical properties. Particularly, we determined the absolute value of the first hyperpolarizability (β) of as-synthesized nano-assembly by the hyper-Rayleigh scattering (HRS) technique and achieved a high value of $\beta = (77 \pm 10) \times 10^{-28}$ esu using 800 nm laser excitation. A transition from non-luminescent to weakly luminescent nanoparticles is observed by adding glutathione as additional capping layer (Cu-Cys-GSH NPs). A strong enhancement of luminescence of Cu-Cys-GSH NPs is observed by using water-ethanol mixture with volume fraction of ethanol 40%. The solvent effect on chiroptical and nonlinear optical properties is also studied. We were also able to measure the two-photon excited PL of Cu-Cys-GSH NPs in water-ethanol mixture because of the strong fluorescence enhancement.

EXPERIMENTAL SECTION

Materials: All the chemicals are commercially available and were used without further purifications. Copper nitrate trihydrate [Cu(NO₃)₂.3H₂O] and sodium hydroxide (NaOH) were purchased from Sigma Aldrich. L-Cysteine was purchased from Acros Organics. L-glutathione (GSH) reduced was procured from Carl Roth. Ethanol and Methanol were purchased from VWR Chemicals and Honeywell, respectively. Ultrapure Milli-Q water (resistivity 18.2 M Ω) was used for all of the experiments.

Synthesis of Self-Assembled Copper Cysteine Nanoparticles (Cu-Cys NP): We have synthesized self-assembled Cu-Cys NPs following an earlier reported protocol with some modification.¹⁵ By using a molar ratio of 2:1 cysteine: Cu²⁺ as initial precursor, the Cu²⁺ is not completely reacted with cysteine ligands. Therefore, we decided to decrease the molar ratio of cysteine: Cu²⁺. Typically, 60.5 mg (0.5 mmol) L-cysteine was dissolved in 5 mL water and then 400 μ L of NaOH (80 mg/mL) was added into the cysteine solution. In another beaker, 241 mg (1 mmol) Cu(NO₃)₂.3H₂O was dissolved in 10 mL water. Then, cysteine solution was added into Cu-solution dropwise and the reaction was continued for at least 30 minutes. The final pH of the solution was in the range of 6.60-6.80. The greyish black colored Cu-Cys NPs were formed and washed by multiple centrifugations.

Purification of Cu-Cys NPs: The as-synthesized Cu-Cys NPs were centrifuged at 6000 rpm (FCR~3180) for 10 minutes. Cu-Cys NPs were precipitated and re-dissolved in water and the

centrifugation process was repeated at least two more times. Then the Cu-Cys NPs were washed with a water-methanol (50:50) mixture. During the centrifugation process, all the unreacted impurities (excess Cu^{2+} , unreacted cysteine and salts) were removed. Then the prepared Cu-Cys NPs were air dried for further use. The dried Cu-Cys NPs were dissolved in 20 mL water for further use (the typical concentration was ~8 mg/mL).

Reaction of Copper-Cysteine NPs with Glutathione: The luminescent Cu-Cys-GSH nano-assemblies were synthesized by the reaction between GSH and Cu-Cys NPs. In a typical reaction, 2 mL Cu-Cys NPs added in 10 mL water and the 1 mL of GSH ligands (30.7 mg/mL) solution added in to it. The reaction was stirred for 30 minutes and the color changed to light yellow (scheme in Figure S1). The nano-assemblies were purified by centrifugation at 15000 rpm for 30 minutes. All the larger NPs, unreacted species were precipitated and discarded. The supernatant solution containing the luminescent Cu-Cys-GSH nano-assemblies was stored at 4°C and then again, we found that larger particles had precipitated. After 24 hours in the solution container, the supernatant was separated by micropipette and used for further investigation.

Instrumentation:

UV-Vis absorption spectra were recorded with an AvaSpec2048FT spectrophotometer, the sample illuminated with continuous spectrum of halogen lamp coupled with AvaLight DH-S deuterium lamp and the transmitted light was collected and analyzed with the spectrophotometer. PL spectra were recorded using a Horiba Jobin Yvon Fluoromax 4 spectrophotometer and the data were collected with FluorEssence software. PL quantum yield (PLQY) was calculated by relative method using the reference dye Coumarin 485 with the following equation:

$$QY_s = \left(\frac{F_s}{F_r} \times \frac{A_r}{A_s} \times \frac{\eta_s^2}{\eta_r^2} \right) \times QY_r \quad (1)$$

F_s and F_r are the integrated fluorescence emission of the sample and the reference, respectively, A_s and A_r are the absorbance at the excitation wavelength of the sample and the reference. QY_s and QY_r (Coumarin 485, 19%) are the quantum yields of the sample and the reference, respectively. Fluorescence lifetime were measured using a custom made set up.²¹ Circular dichroism was recorded by JASCO J815 CD spectropolarimeter.

Morphological studies were performed using transmission electron microscopy (TEM, JEOL-JEM-F2100) at an operating voltage of 200 kV. TEM samples were prepared by drop-

casting solutions onto carbon-coated gold grids. X-ray photoelectron spectroscopy (XPS) (Omicron Nanotechnology instrument) study was carried out to determine the binding energy. Hydrodynamic radius and zeta potential were measured by dynamic light scattering (DLS) using a Malvern Zetasizer Nano ZS. Charge detection mass spectrometry (CDMS) measurements were carried out using a home-built instrument with an electrospray ionization (ESI) source, details description is given elsewhere.²²

Two-photon excited photoluminescence (2-PEPL) cross sections were measured with the relative method using a multiphoton confocal microscope (TE2000-U, Nikon Inc.). The detailed measurement procedure is described in previous paper.²² The 2PEPL cross section was calculated using the following equation with fluorescein dye as reference :

$$\sigma_{2PEPL} = \frac{\eta^{ref} \sigma_2^{ref} c^{ref}}{c} \frac{I}{I_{ref}} \quad (2)$$

where η is the quantum efficiency, σ_2 is the two-photon excited fluorescence cross section, c is the concentration and I is the integrated fluorescence intensity. σ_2 for fluorescein at 780 nm is 33.3 GM.²³ Two-photon absorption (TPA) cross section was calculated by using the following equation.²³

$$\sigma_{TPA} = \frac{\sigma_{2PEPL}}{\phi} \quad (3)$$

Where ϕ is the one-photon QY. We assume that one-photon PLQY = two-photon PLQY as accepted by the photochemistry community with considering Kasha's rule and Vavilov's rule.²³

The hyper HRS set up has been described elsewhere in previous work by Antoine and coworkers.²⁴ The concentration of Cu-Cys-GSH NPs was calculated by extrapolation of mass measurements from CDMS evolution curves with different fraction of ethanol.

RESULTS AND DISCUSSION:

Here we present well-crystallized form Cu-Cys NPs formed from the gradually self-assembled water-insoluble Cys-Cu-Cys molecules (as shown in Scheme 1). The size of as-synthesized Cu-Cys NPs is found to be ~50 nm as shown in figure S2. Cysteine capped Cu-Cys NPs are non-luminescent particles, and these Cu-Cys NPs generate luminescent self-assembled NPs when reacts with glutathione (GSH: a tripeptide molecule consists of glycine, cysteine and

glutamic acid). GSH binds to the Cu-Cys NPs through the thiol end by Cu-S bond formation which is already well established.²⁵

Linear Optical Properties of Cu-Cys-GSH NPs Assembly and the Effect of Ethanol:

The Cu-Cys NPs do not have any characteristic absorption band in the range of 300-500 nm (Figure S3), whereas after GSH attachment to Cu-Cys NPs i.e., in Cu-Cys-GSH NPs a very weak shoulder is found around 335 nm (black line, Figure 1A). The excitation spectrum (blue line) shows a maximum in good agreement with the shoulder presented in absorption profile. The photoemission of Cu-Cys-GSH NPs exhibits a maximum at 623 nm when excited at 380 nm. Moreover, we recorded the excitation dependence over 340-450 nm wavelength range, we did not notice any change in the emission maxima (Figure S4), which may suggest the origin of photoemission is from a single final excited state.

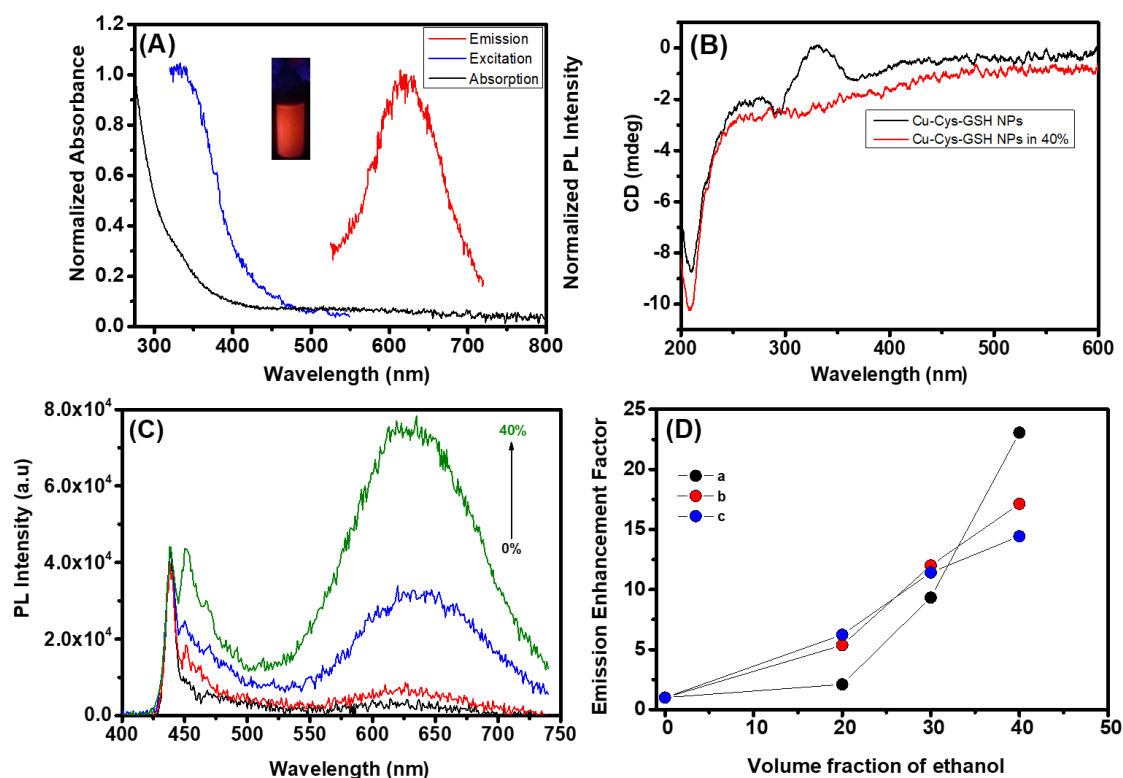


Figure 1. (A) Absorption, emission and excitation spectra of Cu-Cys-GSH NPs, (B) Circular dichroism spectra of Cu-Cys-GSH NPs in water and water-ethanol ($f_e=40\%$) mixture, (C) PL emission enhancement of Cu-Cys-GSH NPs aggregates as a function of volume fraction of ethanol, the other peak at lower wavelength (425-500 nm) is basically the Raman scattering in fluorescence spectra that is coming from solvent (water or water-ethanol mixture). (D) PL

emission stability of Cu-Cys-GSH NPs aggregates with different time intervals, after (a) 30-minutes, (b) 24 hours and (c) 6-days.

We studied the chiroptical properties of NPs, since both the ligands L-Cysteine and L-GSH are chiral ligands. We expect indeed that Cu-Cys-GSH NPs will retain some chiroptical properties too. The circular dichroism (CD) spectra of Cu-Cys-GSH NPs show multiple bands at 209, 292, 332 and 367 nm. The strong negative band at 209 nm is originated from the chiral center of chiral ligands. All other bands are originated due to the development of chiral self-assembled nanostructures from Cys-GSH-Cu(I)/(II) (black line, Figure 1B), displaying chiroptical activities in the near-UV.²⁶ However, we would like point out that both absorption and CD spectra in Ag/Au Cys NPs are drastically different as compared to those reported in this work for Cu-Cys-GSH NPs.^{5, 27} This difference may find its origin in the surface motifs and coordination schemes in the self-assembled NPs. Indeed, the Au/Ag-Cys interaction allows for beta-sheet and alpha-helix structures (since Au/Ag are in the +1-oxidation state) while such structures cannot be observed for Cu-Cys NPs (since the oxidation state is a mixture of +2/+1), see the scheme in Figure S5.

The as-synthesized Cu-Cys-GSH NPs show very weak photoemission band peak at 623 nm with a PLQY of $1.3 \pm 0.2 \times 10^{-2}$ %. Then we tried to enhance the QY of these nano-assembly by further aggregation, which can be controlled by many factors like solvent, metal ion, polymer matrix, and temperature.²⁸⁻³⁰ Interestingly, we found significant enhancement in the luminescence intensity when we changed the solvent polarity by using the less polar ethanol, respective dielectric constant of water and ethanol being, 80.1 and 25.1 at room temperature.³¹ Therefore, we introduced ethanol, into the aqueous solutions of Cu-Cys-GSH NPs with varying volume fraction f_e (where $f_e = V_{\text{ethanol}} / (V_{\text{ethanol}} + V_{\text{water}})$) ranging from 0 to 40% and we observed no change in the emission maxima at 623 nm see Figure 1C. The other peak at lower wavelength (425-500 nm) in fluorescence spectra is the Raman scattering that comes from solvent (water or water-ethanol mixture). We observed PL enhancement with a PLQY of about $9.6 \pm 1.0 \times 10^{-2}$ %, an 8-fold enhancement in QY when f_e increases from 0 to 40% see Figure S6. To check the stability of Cu-Cys-GSH NP, we recorded the absorption spectra of the same in a time interval of seven days and we did not observe any change in the absorption profile which suggest about its good stability (see Figure S7). Noteworthy to mention that in presence of ethanol, the CD signal displayed a weaker chirality for the nano-assembly see Figure 1B (red line). We observed that the PL stability of assembled Cu-Cys NPs aggregates in water-ethanol medium degrades with time. Therefore, we recorded the PL of these systems after 30 minutes,

24 hours and 6 days from sample preparation, see Figure 1D. As the f_e increased, the PL-stability of these aggregates decreased which may be associated with the larger nano-aggregates formation. In addition, we recorded the absorption spectra of Cu-Cys-GSH NPs both in water and mix-solvent of f_e 40% and observed the enhancement of absorbance which can be due to the formation of these larger aggregates, see Figure S8. Moreover, we also tried to induce aggregation using the less polar solvent methanol, see Figure S9. The as-synthesized NPs exhibit large Stokes shift of around 295 nm. To understand the excited state dynamics of the self-assembly Cu-Cys NPs in water and water-ethanol mixtures, we measured the fluorescence lifetime of Cu-Cys-GSH NPs in the respective solvent. The measured lifetime was 214 ± 20 ns in water, which increased to 643 ± 65 ns in presence of 40% ethanol, all the decay curves were fitted bi-exponentially (see Table S1). Therefore, this excited state high lifetime along with large Stokes shift suggests that the origin of this photoemission is associated with a ligand to metal charge transfer (LMCT) involving metal centered triplet states.³¹⁻³³

Non-Linear Optical (NLO) Properties:

We first investigated the NLO properties of Cu-Cys-GSH NPs by measuring the first hyperpolarizability (β) using 800 nm laser excitation. The HRS technique was employed to determine the β value of the self-assembly NPs.^{5, 6} The HRS signal was recorded for various concentrations of NPs in aqueous medium and short-range spectra were recorded in both side of HRS wavelength see Figures 2A-B. The estimated concentration of stock solution of self-assembled NPs is 25 nM based on mass measurements obtained from CDMS. The estimated β value for 800 nm laser excitation is found to $(77 \pm 10) \times 10^{-28}$ esu where we used water as a reference, $\beta_{\text{water}} = 0.087 \times 10^{-30}$ esu. This value is similar order of magnitude as compared to other systems like gold-cysteine.^{5, 6} We also tried to measure the first hyperpolarizability of Cu-Cys-GSH NPs in water-ethanol mixture but observed unstable signal under laser irradiation thus determination of β was not possible.

As the photoemission of assembled Cu-Cys-GSH NPs significantly increased in water-ethanol mixture at $f_e=40\%$, we expected a similar effect for two-photon excited photoluminescence (2PEPL). The 2PEPL spectrum of Cu-Cys-GSH NPs in 40% ethanol exhibit a maximum at 623 nm when excited at 780 nm, whereas the same Cu-Cys NPs self-assembly in water has very weak fluorescence and the 2PEPL cross-section could not be estimated see Figure 2C. We have carried out two-photon fluorescence measurement in

variable excitation power and observed slope ~ 2 for Log (TPEF Intensity) Vs Log (Transmission) plot, which suggests the origin of non-linear two photon fluorescence when excited at 780 nm (see the Figure S10).³⁴ In addition, we carried out HRS experiment with varying excitation power that demonstrated the quadratic behaviour of the process (see the Figure S11). The 2PEPL cross-section of Cu-Cys-GSH NPs in water-ethanol medium at $f_e=40\%$ fraction is estimated as high as 13 ± 2 GM, such value is in similar order of magnitude as compared with other reported system.^{5, 6} Thus, the ethanol induced aggregation has a tremendous impact on two-photon emission and 2PEPL cross-section.

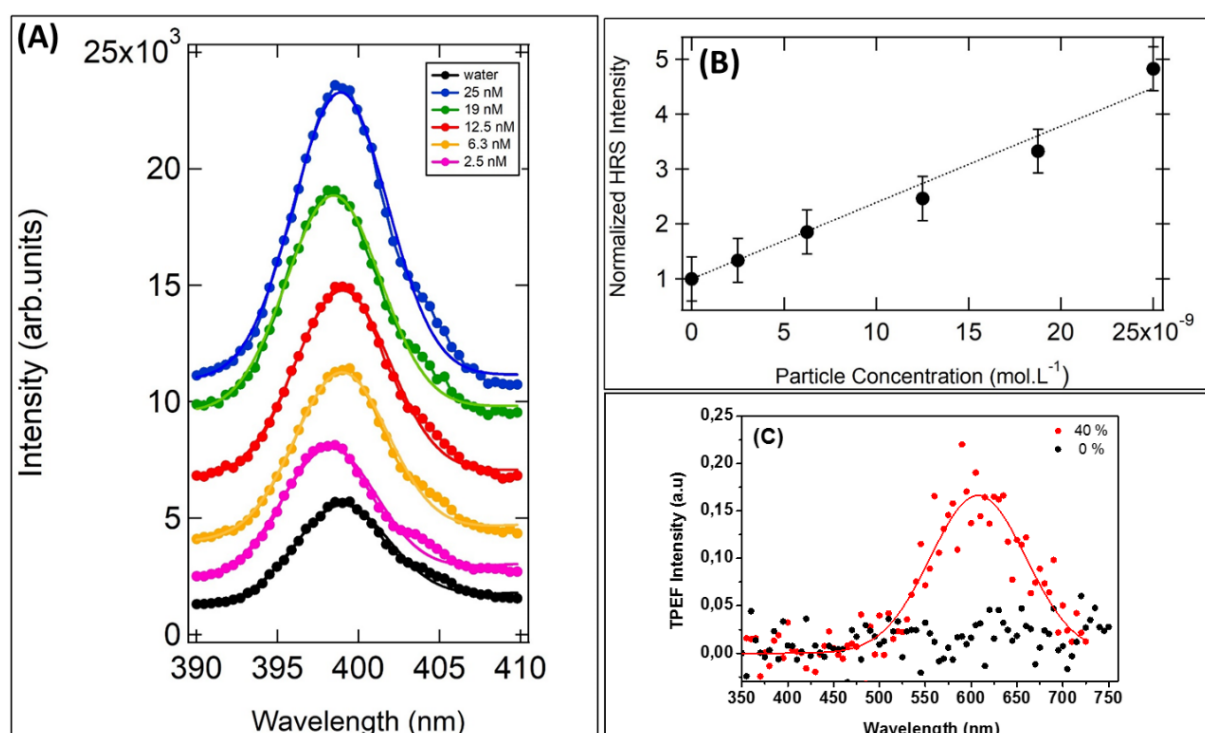


Figure 2. (A) HRS line intensity of Cu-Cys-GSH NPs system with different concentrations. (B) Plot of HRS intensity as a function of concentrations and (C) Two-photon excited fluorescence spectra of Cu-Cys-GSH NPs in water and ethanol-water mixture ($f_e=40\%$).

Structure Optical Properties Relationship and the Effect of Ethanol: When glutathione is reacted with Cu-Cys NPs, polydisperse nano-assemblies in the sub 100 nm were observed (see, Figure 3A). Glutathione is a mild reducing agent, thus can easily react with Cys bounded Cu(II) which results into Cu(I) rich assembly formation as the reaction occurs $[\text{Cu(II)}+\text{GSH} \rightarrow \text{Cu(I)}+\text{GSSG}]$.^{12, 15} Thiolated capped Cu assemblies with rich Cu(I) is known to be luminescent.¹² The emission in Cu-Cys-GSH NPs may be associated with the LMCT from

GSH to Cu ions.¹² However, the redox reaction with GSH occurs with Cu²⁺ ions in isolated solution. Contrary, in our case Cu (II)-ions are already bound with two Cys ligands and the redox properties of Cu will be affected. The main interpretation on how the structure of Cu-Cys-GSH NPs affect the optical properties is rigidification effect. Indeed, since GSH mainly sticks (by covalent and by non-covalent interactions) on the surface of NPs, then a rich H-bound network (between -NH₂ and -COOH surface group) will rigidify the nano-assemblies render them more luminescent (see Figure S12), we have also demonstrated for many systems that luminescence enhancement up on rigidification in the linear optical regime can be translated in nonlinear optical regime.^{35, 36} This behaviour may take origin from the fact that deexcitation pathways are similar up on one and two photons excitations. Now concerning the huge hyperpolarizability value reported for Cu-Cys-GSH NPs, the origin is certainly due to supra-molecular motifs that are highly non-centro symmetric due to the presence of GSH (see Figure S12). Of note, the elemental analysis from EDS data shows that the S-content is 75% after the reaction of Cu-Cys NPs with GSH, which is in favor of an increase of thiol motifs [-GSH-Cu-Cys-Cu-GSH-Cu-] compared to pure Cu-Cys NPs where 41% S-content is observed (see Table S2).

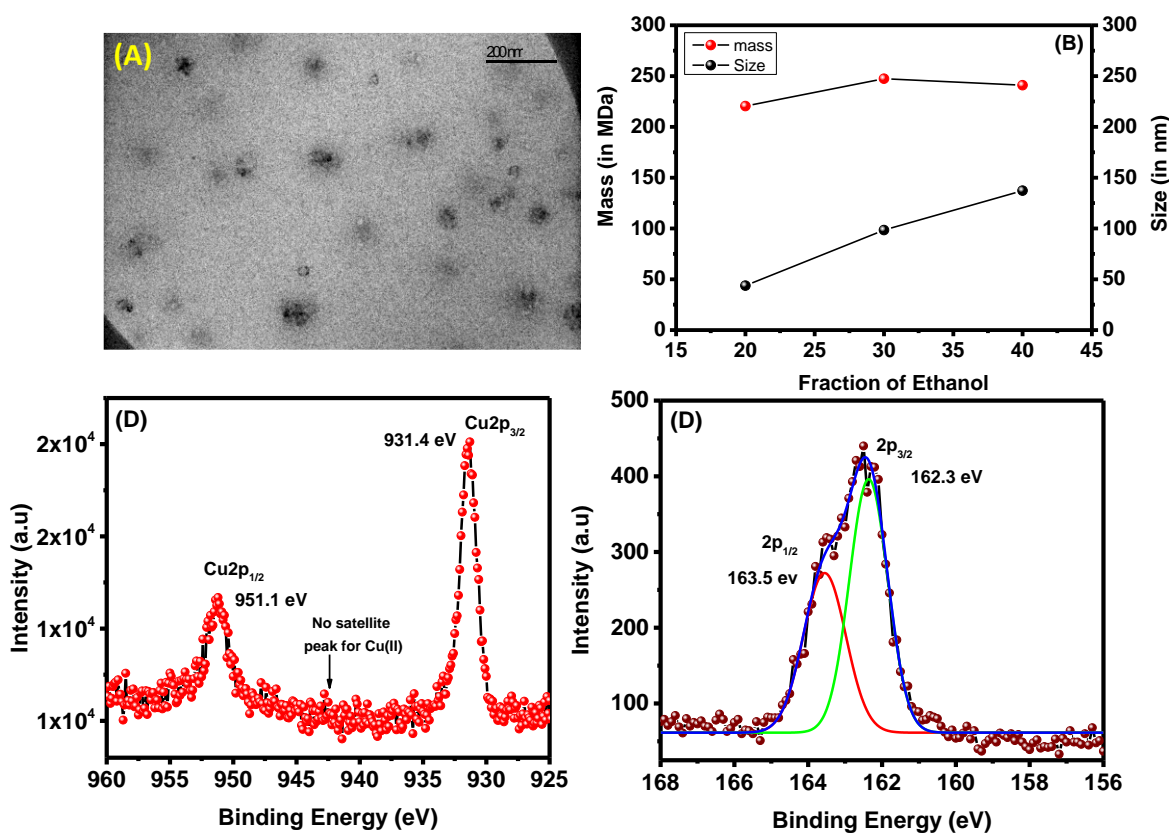


Figure 3. (A) TEM image of Cu-Cys-GSH NPs, (B) estimation of mass of Cu-Cys-GSH NPs nano-assembly with different fractions of ethanol obtained from CDMS measurements with comparing DLS size, XPS spectra of (C) Cu-2p and (D) S-2p of the Cu-Cys-GSH NPs.

In presence of ethanol, the emission enhancement can be explained by AIE which is quite common phenomenon for thiolate protected metal NCs/complexes.^{28, 29} The PL-stability of these aggregates depends on f_e . In particular, above 40% volume fraction of ethanol, the colloidal stability of these aggregates is weaker. To understand this colloidal stability, we measured the zeta potential. For Cu-Cys-GSH NPs without any ethanol, the zeta potential is $(+22.7 \pm 2.3 \text{ mV})$. The zeta potential value decreased to $(+11.4 \pm 2.6 \text{ mV})$ in case of 50% ethanol fraction (Figure S13). In water medium only, the Cu-Cys-GSH NPs show a good stability due to its high surface charge, which helps them to make a good hydration shell with water molecules. When we introduced less polar ethanol in aqueous solution of Cu-Cys-GSH NPs, then ethanol molecules penetrated into the hydration shell of NPs and destroyed the hydration shell that causes the charge neutralization. As a result, the NPs become less stable and form larger particle aggregates. Although the exact mechanism of AIE is not yet clear, probably the solvent-induced aggregation reduced the rotational and vibrational motion of surface ligands Cys and GSH as a result fluorescence emission enhanced in the presence of ethanol.^{29, 31} Again we recorded the TEM image of Cu-Cys-GSH NPs in water-ethanol mixture with 30% ethanol fraction. It is confirmed from the TEM image that Cu-Cys-GSH NPs aggregated in water-ethanol mixture and formed a bulk nanostructure see Figure S14. For further investigation about the size evolution, we recorded the average mass and size of Cu-Cys-GSH NPs particles as a function of ethanol using CDMS and DLS (see Figure 3B). With increasing volume fraction, f_e from 20% to 40%, the average mass of self-assemblies increases from 220 MDa to 241 MDa as surface motifs aggregated and formed larger size self-assemblies. Moreover, we found the mass distribution of these self-assemblies are quite broad from ~ 100 to ~ 600 MDa, see Figure S15. The growing mass in CDMS is further supported by the DLS size measurement where we can see that the size increases from 20 nm to 137 nm when the volume fraction of ethanol is increased from 20 to 40%. Moreover, we have carried out X-ray photon spectroscopy (XPS) investigation to understand the oxidation state of Cu in Cu-Cys-GSH nanoparticles. The peak at 951.1 eV and 931.4 eV are assigned as Cu 2p_{1/2} and Cu 2p_{3/2} respectively (Figure 3C), by comparison with the CuS spectrum.³⁷ No satellite peak present corresponding to 942 eV, indicates the absence of Cu(II) in the paramagnetic chemical state. The binding energy difference between Cu(I) and Cu (0) oxidation state is very less

(about to be 0.1 eV); thus, we can't quantify the amount of Cu(I) or Cu (0) precisely. The binding energy at 162.3 and 163.5 eV are assigned as S 2p_{3/2} and 2p_{1/2} for Cu-S bond which formed upon binding Cu with cysteine and glutathione (Figure 3D).^{25, 38}

CONCLUSION

In summary, we have prepared cysteine protected supramolecular copper nanoparticles (Cu-Cys NPs) which is non emissive. After that, we reacted the Cu-Cys NPs with a tripeptide molecule glutathione which turn on the fluorescence. We have explored the first hyperpolarizability of these Cu based assemblies at 800 nm laser excitation where a large hyperpolarizability value is observed as $(77\pm 10) \times 10^{-28}$ esu. The luminescence of Cu-Cys-GSH NPs may find its origin in the presence of Cu(I) in (-GSH-Cu-Cys-Cu-GSH-Cu-) surface motifs and furthermore we observed that the PL is highly influenced by the solvent polarity of the medium. We found PL enhancement by changing the solvent from pure water to 40% ethanol water-ethanol mixture. Enhancement in PL of NPs in water-ethanol mixture is also observed upon two photon excitations at 780 nm. The present work outlines the unique motifs observed in self-assembled NPs using copper as metal and Cys/GSH as surface ligands. The fact that copper may hold mixture of Cu(I) and Cu(0) oxidation state will lead to unique motifs and metal coordination with thiolates as compared to Ag/Au self-assembled NPs. Future plan may consist in tuning Cu(0) and Cu(I) oxidation state by rational design of thiolates and solvent.

ASSOCIATED CONTENT

Supporting Information: The Supporting Information is available free of charge on the ACS publications website. Synthesis scheme of Cu-Cys-GSH NPs; TEM image; Absorption spectrum; Excitation spectra; Origin of alpha helix and beta sheet; Digital pictures of aggregates; Absorption spectrum of Cu-Cys-GSH; Absorption spectra; PL comparison; Table for lifetime; Log-log plot of the TPEF intensity plot; Dependence of the HRS signal; GSH attachment mechanism; Elemental analysis (EDS); Zeta potential measurement; TEM image of Cu-Cys-GSH in water-ethanol; CDMS histogram;

Notes: The authors declare no competing financial interest.

ACKNOWLEDGMENTS: D.B. is grateful for post-doc fellowship donated by Agence Nationale de la Recherche (project MANBAMM, ANR-21-CE29-0020). H.Y. is grateful for PhD fellowships donated by the China Scholarship Council (CSC, 202206140023). S.M. is grateful for post-doc fellowship donated by the Horizon 2020 Research and Innovation program under grant agreement No. 964553 (project ARIADNE-Vibe). S.K. acknowledges

CEFIPRA for financial support (Raman-Charpak fellowship). R.A. and H.Y. acknowledge Shanghai Science and Technology Innovation Program (22520712500) for support. R.A. acknowledges Agence Nationale de la Recherche (projects MANBAMM, ANR-21-CE29-0020, nanoGOLD, ANR-22-CE29-0022 and MOONSTONE, ANR-22-CE42-0031) for support. R.A., D.B., H.Y., A.P. and J.O.B. acknowledge PHC POLONIUM (Project: 49252PM, “Gold nanoclusters in chiral nano-assemblies - nonlinear optical properties”) for support. R.A., D.B., and S.M. would like to acknowledge X. Dagany, C. Clavier, M. Kerleroux, and G. Montagne for their support in the development of the CDMS setup. In addition, we acknowledge CNRS for funding through International Emerging Actions between France and India.

REFERENCES:

1. Kolay, S.; Bain, D.; Maity, S.; Devi, A.; Patra, A.; Antoine, R., Self-Assembled Metal Nanoclusters: Driving Forces and Structural Correlation with Optical Properties. *Nanomaterials* **2022**, *12*, 544.
2. Basu, S.; Paul, A.; Antoine, R., Controlling the Chemistry of Nanoclusters: From Atomic Precision to Controlled Assembly. *Nanomaterials* **2022**, *12*, 62.
3. Jiang, W.; Qu, Z.-b.; Kumar, P.; Vecchio, D.; Wang, Y.; Ma, Y.; Bahng, J. H.; Bernardino, K.; Gomes, W. R.; Colombari, F. M.; Lozada-Blanco, A.; Veksler, M.; Marino, E.; Simon, A.; Murray, C.; Muniz, S. R.; de Moura, A. F.; Kotov, N. A., Emergence of Complexity in Hierarchically Organized Chiral Particles. *Science* **2020**, *368*, 642-648.
4. Söptei, B.; Mihály, J.; Szigyártó, I. C.; Wacha, A.; Németh, C.; Bertóti, I.; May, Z.; Baranyai, P.; Sajó, I. E.; Bóta, A., The Supramolecular Chemistry of Gold and L-cysteine: Formation of Photoluminescent, Orange-Emitting Assemblies with Multilayer Structure. *Colloids Surf. A: Physicochem. Eng* **2015**, *470*, 8-14.
5. Fakhouri, H.; Perić, M.; Bertorelle, F.; Dugourd, P.; Dagany, X.; Russier-Antoine, I.; Brevet, P.-F.; Bonačić-Koutecký, V.; Antoine, R., Sub-100 Nanometer Silver Doped Gold–Cysteine Supramolecular Assemblies with Enhanced Nonlinear Optical Properties. *Phys. Chem. Chem. Phys.* **2019**, *21*, 12091-12099.
6. Russier-Antoine, I.; Bertorelle, F.; Kulesza, A.; Soleilhac, A.; Bensalah-Ledoux, A.; Guy, S.; Dugourd, P.; Brevet, P.-F.; Antoine, R., Chiral Supramolecular Gold-Cysteine Nanoparticles: Chiroptical and Nonlinear Optical Properties. *Prog. Nat. Sci.: Mater.* **2016**, *26*, 455-460.
7. Kang, X.; Li, Y.; Zhu, M.; Jin, R., Atomically Precise Alloy Nanoclusters: Syntheses, Structures, and Properties. *Chem. Soc. Rev.* **2020**, *49*, 6443-6514.
8. Shen, J.-S.; Li, D.-H.; Zhang, M.-B.; Zhou, J.; Zhang, H.; Jiang, Y.-B., Metal–Metal-Interaction-Facilitated Coordination Polymer as a Sensing Ensemble: A Case Study for Cysteine Sensing. *Langmuir* **2011**, *27*, 481-486.
9. Randazzo, R.; Di Mauro, A.; D’Urso, A.; Messina, G. C.; Compagnini, G.; Villari, V.; Micali, N.; Purrello, R.; Fragalà, M. E., Hierarchical Effect behind the Supramolecular

Chirality of Silver(I)–Cysteine Coordination Polymers. *J. Phys. Chem. B* **2015**, *119*, 4898-4904.

10. Veselska, O.; Podbevšek, D.; Ledoux, G.; Fateeva, A.; Demessence, A., Intrinsic Triple-Emitting 2D Copper Thiolate Coordination Polymer as a Ratiometric Thermometer Working Over 400 K Range. *Chem. Commun.* **2017**, *53*, 12225-12228.

11. Zhao, S. S.; Wang, L.; Liu, Y.; Chen, L.; Xie, Z., Stereochemically Dependent Synthesis of Two Cu(I) Cluster-Based Coordination Polymers with Thermochromic Luminescence. *Inorg. Chem.* **2017**, *56*, 13975-13981.

12. Yin, S.-N.; Liu, Y.; Zhou, C.; Yang, S., Glutathione-Mediated Cu(I)/Cu(II) Complexes: Valence-Dependent Effects on Clearance and In Vivo Imaging Application. *Nanomaterials*, **2017**, *7*, 132.

13. Deng, S.-Q.; Mo, X.-J.; Cai, S.-L.; Zhang, W.-G.; Zheng, S.-R., Homochiral Cu(I) Coordination Polymers Based on a Double-Stranded Helical Building Block from Achiral Ligands: Symmetry-Breaking Crystallization, Photophysical and Photocatalytic Properties. *Inorg. Chem.* **2019**, *58*, 14660-14666.

14. Dokken, K. M.; Parsons, J. G.; McClure, J.; Gardea-Torresdey, J. L., Synthesis and Structural Analysis of Copper(II) Cysteine Complexes. *Inorg. Chim. Acta* **2009**, *362*, 395-401.

15. Ma, B.; Wang, S.; Liu, F.; Zhang, S.; Duan, J.; Li, Z.; Kong, Y.; Sang, Y.; Liu, H.; Bu, W.; Li, L., Self-Assembled Copper–Amino Acid Nanoparticles for in Situ Glutathione “AND” H₂O₂ Sequentially Triggered Chemodynamic Therapy. *J. Am. Chem. Soc.* **2019**, *141*, 849-857.

16. Luo, Z.; Yuan, X.; Yu, Y.; Zhang, Q.; Leong, D. T.; Lee, J. Y.; Xie, J., From Aggregation-Induced Emission of Au(I)–Thiolate Complexes to Ultrabright Au(0)@Au(I)–Thiolate Core–Shell Nanoclusters. *J. Am. Chem. Soc.* **2012**, *134*, 16662-16670.

17. Tan, H.; Zhou, H.; Zhao, Y.; Wang, X.; He, X.; Chen, J.; Zhang, K.; Antoine, R.; Zhang, S.; Tian, Y., Regulation of Silver Nanoclusters with 4 Orders of Magnitude Variation of Fluorescence Lifetimes with Solvent-Induced Noncovalent Interaction. *J. Phys. Chem. C* **2022**, *126*, 5198-5205

18. Deng, H.-H.; Shi, X.-Q.; Peng, H.-P.; Zhuang, Q.-Q.; Yang, Y.; Liu, A.-L.; Xia, X.-H.; Chen, W., Gold Nanoparticle-Based Photoluminescent Nanoswitch Controlled by Host–Guest Recognition and Enzymatic Hydrolysis for Arginase Activity Assay. *ACS Appl. Mater. Interfaces* **2018**, *10*, 5358-5364.

19. Deng, H.-H.; Shi, X.-Q.; Wang, F.-F.; Peng, H.-P.; Liu, A.-L.; Xia, X.-H.; Chen, W., Fabrication of Water-Soluble, Green-Emitting Gold Nanoclusters with a 65%

Photoluminescence Quantum Yield via Host–Guest Recognition. *Chem. Mater.* **2017**, *29*, 1362-1369.

20. Pniakowska, A.; Samoć, M.; Olesiak-Bańska, J., Strong Fluorescence-Detected Two-Photon Circular Dichroism of Chiral Gold Nanoclusters. *Nanoscale* **2023**, *15*, 8597-8602.

21. Soleilhac, A.; Dagany, X.; Dugourd, P.; Girod, M.; Antoine, R., Correlating Droplet Size with Temperature Changes in Electrospray Source by Optical Methods. *Anal. Chem.* **2015**, *87*, 8210-8217.

22. Basu, S.; Fakhouri, H.; Moulin, C.; Dolai, S.; Russier-Antoine, I.; Brevet, P.-F.; Antoine, R.; Paul, A., Four Orders-of-Magnitude Enhancement in the Two-Photon Excited Photoluminescence of Homoleptic Gold Thiolate Nanoclusters following Zinc Ion-Induced Aggregation. *Nanoscale* **2021**, *13*, 4439-4443.

23. Fakhouri, H.; Salmon, E.; Wei, X.; Joly, S.; Moulin, C.; Russier-Antoine, I.; Brevet, P.-F.; Kang, X.; Zhu, M.; Antoine, R., Effects of Single Platinum Atom Doping on Stability and Nonlinear Optical Properties of Ag₂₉ Nanoclusters. *J. Phys. Chem. C* **2022**, *126*, 21094-21100.

24. Russier-Antoine, I.; Fakhouri, H.; Basu, S.; Bertorelle, F.; Dugourd, P.; Brevet, P.-F.; Velayudhan, P.; Thomas, S.; Kalarikkal, N.; Antoine, R., Second Harmonic Scattering from Mass Characterized 2D Graphene Oxide Sheets. *Chem. Commun.* **2020**, *56*, 3859-3862.

25. Maity, S.; Bain, D.; Patra, A., Engineering Atomically Precise Copper Nanoclusters with Aggregation Induced Emission. *J. Phys. Chem. C* **2019**, *123*, 2506-2515.

26. Chang, H.-Y.; Tseng, Y.-T.; Yuan, Z.; Chou, H.-L.; Chen, C.-H.; Hwang, B.-J.; Tsai, M.-C.; Chang, H.-T.; Huang, C.-C., The Effect of Ligand–Ligand Interactions on the Formation of Photoluminescent Gold Nanoclusters Embedded in Au(I)–Thiolate Supramolecules. *Phys. Chem. Chem. Phys.* **2017**, *19* (19), 12085-12093.

27. Řezanka, P.; Záruba, K.; Král, V., Supramolecular Chirality of Cysteine Modified Silver Nanoparticles. *Colloids Surf. A: Physicochem. and Eng.* **2011**, *374*, 77-83.

28. Luo, Z.; Yuan, X.; Yu, Y.; Zhang, Q.; Leong, D. T.; Lee, J. Y.; Xie, J., From Aggregation-Induced Emission of Au(I)–Thiolate Complexes to Ultrabright Au(0)@Au(I)–Thiolate Core–Shell Nanoclusters. *J. Am. Chem. Soc.* **2012**, *134*, 16662-16670.

29. Goswami, N.; Yao, Q.; Luo, Z.; Li, J.; Chen, T.; Xie, J., Luminescent Metal Nanoclusters with Aggregation-Induced Emission. *J. Phys. Chem. Lett.* **2016**, *7*, 962-975.

30. Bera, D.; Goswami, N., Driving Forces and Routes for Aggregation-Induced Emission-Based Highly Luminescent Metal Nanocluster Assembly. *J. Phys. Chem. Lett.* **2021**, *12*, 9033-9046.

31. Bain, D.; Maity, S.; Patra, A., Surface Motifs Regulated Aggregation Induced Emission in Gold–Silver Nanoclusters. *Chem. Commun.* **2020**, *56*, 9292-9295.
32. Wu, Z.; Jin, R., On the Ligand's Role in the Fluorescence of Gold Nanoclusters. *Nano Lett.* **2010**, *10*, 2568-2573.
33. Huang, Y.; Fuksman, L.; Zheng, J., Luminescence Mechanisms of Ultrasmall Gold Nanoparticles. *Dalton Trans* **2018**, *47*, 6267-6273.
34. Gálico, D. A.; Ovens, J. S.; Sigoli, F. A.; Murugesu, M., Room-Temperature Upconversion in a Nanosized {Ln₁₅} Molecular Cluster-Aggregate. *ACS Nano* **2021**, *15*, 5580-5585.
35. Perić, M.; Sanader Maršić, Ž.; Russier-Antoine, I.; Fakhouri, H.; Bertorelle, F.; Brevet, P.-F.; le Guével, X.; Antoine, R.; Bonačić-Koutecký, V., Ligand Shell Size Effects on One- and Two-Photon Excitation Fluorescence of Zwitterion Functionalized Gold Nanoclusters. *Phys. Chem. Chem. Phys.* **2019**, *21*, 23916-23921.
36. Bertorelle, F.; Moulin, C.; Soleilhac, A.; Comby-Zerbino, C.; Dugourd, P.; Russier-Antoine, I.; Brevet, P.-F.; Antoine, R., Bulky Counterions: Enhancing the Two-Photon Excited Fluorescence of Gold Nanoclusters. *ChemPhysChem* **2018**, *19*, 165-168.
37. Wu, Z.; Liu, J.; Gao, Y.; Liu, H.; Li, T.; Zou, H.; Wang, Z.; Zhang, K.; Wang, Y.; Zhang, H.; Yang, B., Assembly-Induced Enhancement of Cu Nanoclusters Luminescence with Mechanochromic Property. *J. Am. Chem. Soc.* **2015**, *137*, 12906-12913.
38. Gao, X.; Lu, Y.; Liu, M.; He, S.; Chen, W., Sub-Nanometer Sized Cu₆(GSH)₃ Clusters: One-Step Synthesis and Electrochemical Detection of Glucose. *J. Mater. Chem. C* **2015**, *3*, 4050-4056.